Improving Propagation Modeling in Urban Environments for Vehicular Ad Hoc Networks

Seyed A. Hosseini Tabatabaei, Martin Fleury, *Member, IEEE*
Nadia N. Qadri, *Student Member, IEEE* and Mohammed Ghanbari, *Fellow, IEEE*

***Abstract*—** Developing applications, especially real-time ones, for wireless vehicular ad hoc networks (VANETs) requires a reasonable assurance of the likely performance of the network, at the least in terms of packet loss ratios and end-to-end delay. Because wireless propagation strongly influences performance, especially in an urban environment, this paper improves on simpler propagation models for simulations by augmenting ray-tracing derived models of propagation. In the non-line-of-sight component: the propagation distance is more closely calculated according to the reflection distance; the effect of roadside obstacles is included; and for modeling of fast fading a phase factor is introduced, all without necessarily overly increasing computational load. In the line-of-sight component, as well as roadside obstacle modeling: single and double reflections from roadside buildings are added to the standard two-ray ground-propagation model; the distribution of vehicles within a street segment is used to model the ground reflection ray more closely; and the reflection coefficient is also adjusted accordingly to account for reflections from vehicles. The results have been compared with widely-used measurement studies of city streets in the literature, which have confirmed the overall advantage of the improvements, especially in the case of the non-line-of-sight component. A simulation case study shows that in general optimistic performance predictions of packet loss occur with the two-ray ground propagation model when indiscriminately applied. The paper, therefore, represents a way forward for VANET wireless channel modeling in simulations.

Index Terms—simulation, urban environment, vehicle-to-vehicle communication, wireless propagation

I. INTRODUCTION

GENERAL-purpose or generic ad-hoc network simulations have tended to restrict modeling of the wireless path loss to simpler models. These models do not consider environment characteristics that determine the effects of: shadowing caused by obstacles on the path which may cause absorption; reflection; diffraction; and scattering, as generally occurs, especially in a built environment. In addition, multipath effects give rise to fast fading. For perhaps a typical example, at least in the use of the simpler two-ray ground-propagation model in an ns2 simulation, consider the research reported in [1], which, by employing GPS, implies an outdoor environment for the vehicles concerned. In an outdoor environment, the environment characteristics already mentioned may come into play. Of course, in generic ad hoc network modeling as in [1], the conditions of the simulation may well be sufficient. However, in general, incorrect modeling of the physical layer [2] will affect all higher layers. For instance, if a protocol relies on a distance calculation (by inputting a Received Signal Strength Indicator value) based on an incorrect equation for propagation then its simulated performance could be reported incorrectly. In [3], it was shown that modeling of ad hoc routing protocols at higher layers of the protocol stack but neglecting physical layer modeling could give misleading rankings of the protocols. The work in [4] also highlighted the shortcomings of the well-known ns2 simulator for ad hoc wireless modeling and considered various channel error models, though for indoor environments, which are not usually applicable to VANETs. In [5], the effect on VANET ns2 simulations was considered if buildings were to block all but line-of-sight (LOS) communication. The number of 'blind' vehicles increased but the risk of broadcast storms decreased. However, in [5] it was assumed that only LOS took place at the frequency of interest, 5.9 GHz, whereas measurements at this frequency in the streets of Detroit and Michigan [6] showed that non-line-of-sight (NLOS) communication did take place in the presence of tall buildings.

Simulation is the main tool for research on VANETs [8], because the complex vehicle mobility models that arise are unlikely to be represented analytically. There are a large number of variables (vehicle density, car speeds, driver behavior, road obstacles, road topologies …) and it is difficult to conduct repeated live experiments. While improved models for driver behavior are increasingly available [7] [8] [9], it is not clear whether wireless shadowing and fading have been adequately incorporated into the path loss models of current simulators. Models based on ray optics and Fresnel-Kirchoff diffraction theory have shown good path loss accuracy when compared to measurement data within an urban environment [10] [11] [12]. The main obstacle to their incorporation into simulators is the high computation and memory requirements these models generate [10], which means that, hitherto, their main use has been in positioning base stations within urban microcells. In [13], to avoid the need for detailed information about buildings and to reduce excessive computation, a modified version of the complex Kaji propagation model for vehicles with low-height antennas resulted in a computational saving of approximately one third. The accuracy was reported [12] to still be about 80%, though without evaluation against measurement data.

Empirical models based on measured data such as [14] are also unsuitable in a simulator for a number of reasons. They may rely on a flat terrain, or they may be frequency dependent, or when developed for microcells assume roof-top reflections [15] rather than the multiple reflections against buildings and diffractions around street corners that occur

Manuscript received July 31, 2009. This work was supported in part by the COMSTAS Institute of Technology, Islamabad, Pakistan. The authors are with the University of Essex, School of Computer Science and Electronic Engineering, Wivenhoe Park, Colchester CO4 3SQ, UK, (e-mails: amirtaba@hotmail.com {fleum, nnawaz, ghan} @ essex.ac.uk). Corresponding author: M. Fleury phone: +44 1206-872-817; fax: +44 1206-872-900; e-mail: fleum @ essex.ac.uk; fleury.martin55@gmail.com.

when antennas are at street level.

However, research in [16] presented computationally tractable analytical equations for NLOS propagation, based on simplifying assumptions for equations in earlier work [10] for low antennas at lamp-post level. In these equations, reflection loss is constant and there is a single dominant reflection path and a single direct diffraction path. Because, in NLOS modeling, it has been found that ground reflection can be neglected [10] [16], a 2D model is employed. Nevertheless, we have noticed that these equations do not properly estimate the propagation path distance; neglect the effect of scattering from roadside obstacles to propagation (the 'foliage effect') and in general average out constructive and destructive phase effects, which cause fast fading. The net result is that there is a loss in accuracy that could be avoided without a significant computational cost. Notice that estimating phase effects is an alternative to modeling by 'worst-case' Rayleigh or Rician probability density distributions [2], which may incur a computational penalty. Many other models are also feasible [17] such as Log-Normal and Nakagami [18] but our paper concentrates on ray-tracing derived models.

Therefore, it is possible to improve the accuracy of the equations for VANET modeling while still allowing them to be incorporated into widely-available simulators such as Global Mobile System Simulator (GloMoSim) [19]. The equations represent communication from one vehicle to another in a side street and from one vehicle to another in a parallel street (assuming a Manhattan grid type road topology [20]). It is in NLOS modeling that the largest improvements are likely, because in LOS modeling [21] especially in rural areas, the interference between the direct path and the path reflected from the road dominates. In essence, the main contributions of this paper to NLOS modeling are 1) modification of the total propagation path given in [16] during multiple reflections 2) adding the effect of phase distortion, and 3) from [21] adding the effect of scattering by roadside obstacles.

This paper also presents improved modeling of LOS modeling that includes car clustering at junctions, the effect of different reflectivity depending on whether the 'ground' surface is a car or asphalt (road surface), 'foliage' effects from high-positioned obstacles, and phase effects (the latter also present in NLOS modeling). Though the two-ray ground propagation model may be appropriate in rural areas, it has long been known [22] that a six-ray model in urban areas (ones with high-rise buildings acting as reflectors) for LOS is more appropriate, as it takes account of the effect of road width.

These propagation models along with driver behavior modeling from VanetMobiSim [9], allow more accurate VANET simulations in GloMoSim. In addition, there are also simulators under development [8] by the vehicle manufacturers. Therefore, these simulators with improved propagation models represent a way forward in VANET modeling and research. Section II now details the improvements to the equations for NLOS and changes to the two-ray model for LOS propagation. That Section compares the new equations with measured data and the previous equations from which the improvements have evolved. Section III is a simulation case study, the purpose of which is to illustrate how the combination of the NLOS and LOS components in a 'multi-ray' model results in more pessimistic estimates of packet loss, end-to-end delay and packet overhead. This is because of the impact of propagation on the routing model itself. Section IV concludes the paper by assessing the gain from using the multi-ray model.

II. IMPROVEMENTS TO ANALYTICAL EQUATIONS

A number of available measurement studies [22] were carried out in the cellular band at 900 MHz and were used as a point of comparison by others [10][14], whereas Dedicated Short Range Communications (DSRC) devices [23] at the data-link and physical layers under IEEE 802.11p [24] operate at 5.9 GHz. Therefore, before proceeding one should consider how relevant are these measurement studies to the new band? One of the main advantages of an analytical model compared to a model based on measurements (refer back to Section I) is that it is not frequency dependent. In the other words, the presentation in this Section considers the dominant rays after reflections, diffractions and scattering in each path regardless of a particular frequency. Because the equations are mostly parameterized by frequency, changing the frequency does not invalidate the equations. The dominant rays will be weighted based on the frequency of interest and the distance to the receiver. This assumption while direct propagation in the NLOS model is possible but will become invalid when direct propagation is no longer possible. This will occur at much lower frequencies than 900 MHz and is not a problem at higher frequencies such as 5.9 GHz.

However, to reduce computational complexity a constant reflection loss was introduced in equation (1) in Section II.A. The value was assigned empirically from [16] and evaluation in the range 900 MHz to 5.3 GHz shows that this constant produces good results. However, should the reader prefer in their own modelling to adapt the formulas in Section II.A, then equation (20) is available for frequency-sensitive reflection loss. In fact, in the LOS equations of Section II.B, equations parameterized by frequency for reflection loss are employed. In the case of the foliage effect employed in the NLOS and LOS modelling, this is independent of frequency and has been tested in [21] for 457 MHZ and 10.7 GHz, which implies the effect will also hold for 5.9 GHz, as this frequency lies between these frequencies.

In summary, for analytical equations whenever there is a frequency component in the equations then validating the equations against measurements at one frequency (for practical reasons) serves to validate the equations at other frequencies.

A. NLOS modeling

The computationally-tractable, path-loss equations presented in [16] for path-loss prediction are based on calculating path loss by the dominant reflection path and direct diffraction path. In the case of diffracted rays, only direct diffraction from transmitter to receiver vehicles is taken into account and, for multiple reflections, only the signal attenuation over the ray with a minimum number of reflections is investigated. The

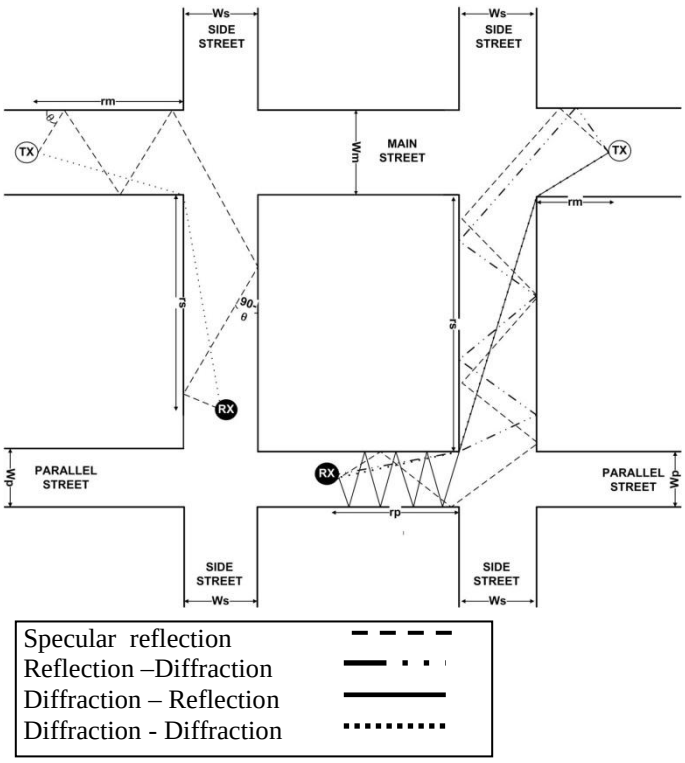

Fig. 1. Transmission paths from a transmitter (tx) to a receiver (rx) in a side street and from a transmitter and receiver in a parallel street.

model assumes [16] that tall buildings with uniform flat surfaces border the streets. As a practical measure, permittivity and conductivity are set as constant values, the result of averaging across the surface of a building. Therefore, there is no diffuse scattering from the surface of buildings and no changes to the polarization of the electromagnetic wave. As with many models for mobile signal strength attenuation, account is not taken of environmental attenuation that occurs at high frequencies in the presence of precipitation and aerosols or, more generally, whenever the wavelength of the wireless signal is of the same scale as an obstacle, which is likely at high frequencies. As elsewhere, Doppler spread is neglected and in fact it is reported to be small in these environments [25], though Doppler spread is an issue at the high speeds of highways [6]. Building plan geometry can also be introduced into a simulation [26], though the work in [26] does not validate their dual-slope channel model against measured data. Fig. 1 shows the geometry referred to in the following discussion for NLOS transmission to a vehicle in a side street and transmission to a vehicle in a parallel street. Notice that there are reflection-diffraction, diffraction-diffraction, and diffraction-reflection components in transmission to a parallel street. In the following, for ease of description, the main discussion is restricted to modifications to the side street communication.The equation [16] for the reflection path loss component (in units of dB) of a signal passing from a vehicle positioned at the center of a main street to one in the center of a side street leading off the main street is:

$$PL_R = 10\log\left(\frac{\lambda}{4\pi(r_m + r_s)}\right)^2 + L_W N_{\min} \quad (1)$$

and for the diffraction component:

$$if\ (r_M > r_S)$$

$$PL_D = 10\log\left(\left(\frac{\lambda}{4\pi r_m}\right)^2\right) + 10\log\left(\frac{\lambda r_m}{4r_s^2}\right) \quad (2)$$

$$if\ (r_s > r_m)$$

$$PL_D = 10\log\left(\left(\frac{\lambda}{4\pi r_s}\right)^2\right) + 10\log\left(\frac{\lambda r_s}{4r_m^2}\right) \quad (3)$$

where r_m is the distance from the transmitting vehicle to the junction of the side street with the main street; r_s is the distance from the junction along the side street to the receiving vehicle; and the reflection loss due to absorption. $L_w = 20logR_o$. R_0 is a constant reflection coefficient. R_0 is assumed to be the same value for side street and main street. $N_{min}$is the minimum number of reflections in any path from the transmitter to the receiver. Notice that research in [11] reports that positioning of the vehicle in the center of a street only influences the results to a very small extent. The first term in (1) is the free space propagation loss which is frequency dependent via the wavelength λ, while the second term represents the loss along the streets (main and side) formed by multiplying the minimum number of reflections by the loss from absorption.

The diffraction component equations (2) and (3) are untouched by us, though we note that it is possible to improve the diffraction near to the junction by means of the Uniform Theory of Diffraction, as reported in [27]. However, the free-space propagation term does not accurately account for the distance traveled by the signal. It assumes that this is the same as the total length of the two streets, whereas the reflections from side to side of the street cause this distance to be changed. In fact, the width of streets is also important because there will be more reflections in a narrower street than there will be in a wider street, again resulting in different signal propagation distances. The free-space loss of the signal due to its expansion during propagation is proportional to the square of the distance. Therefore, accurate calculation of the propagation distance in a simulation has an important influence, especially when specular reflected rays are the dominant received signal. It is also possible to adjust the model for reflections at non-perpendicular road junctions but unless building maps are used in the simulation this does not appear to be an issue.

For a side street, the distances along the main and side streets are better represented as:

$$r_{tm} = \sqrt{\frac{r_m(r_m w_s + r_s w_m)}{w_s}} \quad (4)$$

$$r_{ts} = \sqrt{\frac{r_s(r_m w_s + r_s w_m)}{w_m}} \quad (5)$$

where w_s is the (constant) width of the side street and w_m is the constant width of the main street. Similarly, for transmission to a vehicle in a parallel street

$$r_{tm} = \left(\left(\frac{r_m}{w_m}\right) + \left(\frac{r_p}{w_p}\right) + \left(\frac{r_s}{w_s}\right)\right)\left(r_m \sqrt{w_s w_p w_m \Big/ r_s(w_m r_p + w_p r_m)}\right) \quad (6)$$

$$r_{ts} = \left(\left(\frac{r_m}{w_m}\right) + \left(\frac{r_p}{w_p}\right) + \left(\frac{r_s}{w_s}\right)\right)\sqrt{\frac{w_s r_s}{\left(\frac{r_m}{w_m}\right) + \left(\frac{r_p}{w_p}\right)}} \quad (7)$$

$$r_{tp} = \left(\left(\frac{r_m}{w_m}\right) + \left(\frac{r_p}{w_p}\right) + \left(\frac{r_s}{w_s}\right)\right)\left(r_p \sqrt{w_s w_p w_m \Big/ r_s(w_p r_m + w_m r_p)}\right) \quad (8)$$

where r_p and w_p are the distance along the parallel street and the (constant) width of the parallel street respectively. In Fig. 2, W is the width of a street, R is the reflected distance, r is the projection of R upon the roadside building, and θ is the angle of incidence. With perfect reflection the angle of incidence is the same as the angle of reflection. From [16] or by derivation

$$N_{min} = \left\lfloor 2\sqrt{\frac{r_m r_s}{w_m w_s}} \right\rfloor, \quad (9)$$

where $\lfloor x \rfloor$ is the nearest integer below x. From the geometry of Fig. 2, $R = w/\cos\theta$ and, therefore, the desired total reflection path distance is $N_{min}.w/\cos\theta$. The values (4) to (8) are then found for each street in this way.

These adjusted distances are now applied to the reflection path component of (1) as

$$PL_R = 10\log\left(\frac{\lambda}{4\pi(r_{tm} + r_{ts})}\right)^2 + L_W N_{\min} \quad (10)$$

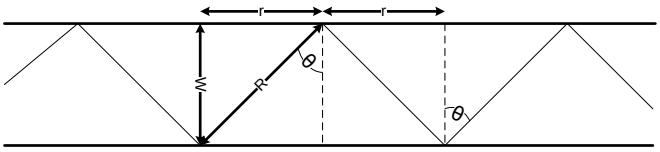

Fig. 2. Geometry for calculating reflection distance, *R*

and the reflection-reflection component of transmission to a parallel street as:

$$PL_{RR} = 10\log\left(\frac{\lambda}{4\pi(r_{tm} + r_{ts} + r_{tp})}\right)^2 + L_W N_{\min} \quad (11)$$

However, equations (10) and (11) suffer from lack of information about the scattering and fading effect of roadside obstacles. In work by Oda et al. [21] it was shown that significant improvement in calculating the path loss arises from considering high-positioned roadside obstacles. The other important factor that is neglected in (10) and (11) is the effect of different rays' phase combination. This will result in significant changes to path loss when the amplitudes of different paths are close to each other. Phase effects also result in fluctuation of the signal according to the distance travelled by the signal, i.e. fast fading.

In our formulation, the effect of scattering and shadowing by roadside obstacles, as typically occurs due to roadside trees, signs, and traffic signals is (multiplicatively) applied to (10) and (11) using the equation in [18], reproduced as (12). The collision probability in this equation is determined by the density of obstacles in high positions between transmitting and receiving vehicles. According to [21], the 'foliage' effect can be applied to the equations by means of the visibility factor, *P*, as follows:

$$P(r) = e^{-sr} \quad (12)$$

where s is the collision probability and r is the distance between transmitter and receiver, which varies according to whether the component is diffracted or reflected. Proposed values [21] for s are 0 for an open area and 0.002 for an urban area (in Tokyo).

When a number of rays from different paths are received with different phase the combined result can be constructive or destructive depending on phase difference (a cause of short-range fading). As mentioned, this effect is significant when the magnitude of the signals over the different paths is comparable. For specular reflected rays the phase part of the field can be estimated by the following equation:

$$\exp\left(-i(k(r_{ts} + r_{tm}) + N_{min}.\pi\right) \quad (13)$$

where k is the wave number. In addition, for a diffracted signal the field phase change can be estimated by:

$$\exp\left(-i\big(k(r_s + r_m)\big)\right) \quad (14)$$

In (14), the original distances from [16] are retained, as the diffraction equations are not altered by us.

Application of these phase components to calculation of the loss is illustrated in [28], for example the electric reflected field becomes:

$$Er = (R_0^{N_{\min}})\left(\frac{e^{-i(k(r_{ts}+r_{tm}+N_{\min}\cdot\pi))}}{r_{ts}+r_{tm}}\right) \quad (15)$$

and the electric diffracted field becomes:

$if\ (r_m > r_s)$

$$\mathrm{Ed} = \left(\left(\frac{i}{4\lambda}\right)\left(A\frac{e^{(-ik(r_m+r_s))}}{r_m r_s}\right)2\lambda\,(\lambda r_s)^{.5}\right) \quad (16)$$

$if\ (r_m < r_s)$

$$Ed = \left(\left(\frac{i}{4\lambda}\right)\left(A\frac{e^{(-ik(r_m+r_s))}}{r_m r_s}\right)2\lambda(\lambda r_m)^{.5}\right) \quad (17)$$

so that:

$$L = 20\log\left(\left(\frac{\lambda}{4\pi}\right)\left|\frac{Etot}{E_0}\right|\right), \quad (18)$$

where *Etot=Er + Ed*.

Fig. 3 compares application of the equations in [16] with a version of the equations (F1) that includes more accurate calculation of the propagation distance and the effect of 'foliage' but does not include the impact of phase change. Specifically, F1 includes equations (10) to (12) which replace the equivalent equations in [16]. For example, as previously stated, equation (10) replaces equation (1), which originates from [16]. (The original measurements in feet are retained for comparison with other works that use this data. 1 ft = 0.3048 m.) Fig. 4 also includes calculation of phase change in a revised equation (F2). Specifically, in addition to the versions of the equations in F1, F2 includes a phase loss factor given by equation (18). The measured data from [22] quoted in [14] [16] are the mean attenuation of transmission (at 894 MHz) along the 51st Avenue (side street) of Manhattan, New York, from its junction with Lexington Avenue (main street). The value of the collision probability was set to s = 0.001 to reflect the reduced density of high-position road side obstacles in New York relative to Tokyo. In general, the loss predicted by [16] is less than that of the equations presented in this paper. Because the distance along the Avenue has not changed

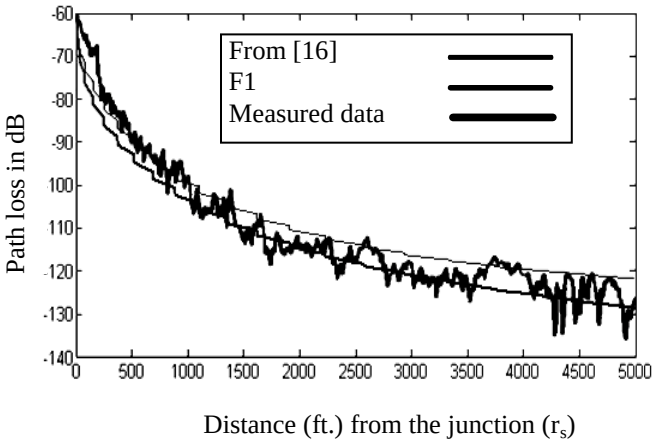

Fig. 3. Comparison of the equations for side-street path loss, from [16] and the revised equation (F1) including accurate calculation of propagation distance and 'foliage' effect, with measured data from [22], settings — frequency = 900 MHz, *rm* = 39.2 m, *Wm* = 28.6 m, *Ws* = 20.4 m, *s* = 0.001

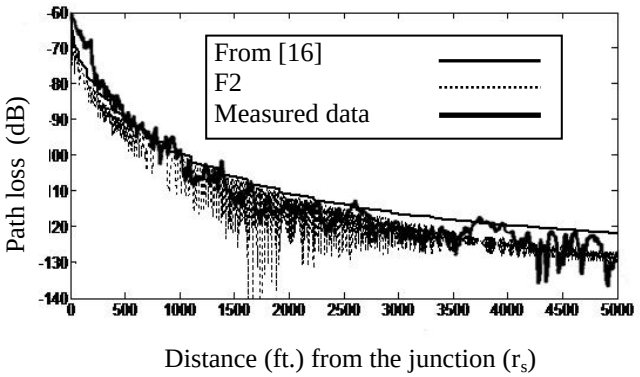

Fig. 4. Comparison of the equations for side-street path loss, from [16] and the revised equation (F2) including accurate calculation of propagation distance, 'foliage' effect, and phase change, with measured data from [22], settings — frequency = 900 MHz, *rm* = 39.2 m, *Wm* = 28.6 m, *Ws* = 20.4 m, *s* = 0.001

noticeably for r_s up to about 900 ft the effect of improved distance calculation does not occur. The reflected component is also becomes dominant over the diffracted component from 2000 ft. Therefore, the equation from [16] is nearer to the measured path loss, though all equations are in reasonable agreement, with estimation error greatest at short distances. However, from about 900 ft onwards the equation in [16] is unable to follow the increase in losses. From 2000 ft onwards the 'foliage' effect has an increased impact while the reflected component weakens relative to the diffracted component.

As an additional example, in a detailed comparison between measured data and simulation [28] for path loss after transmission along Stadiou Street (side street)[1] in Athens, Greece, it was found that a mean square error offset (9.4 dB in [28]) adjusted simulated results to the measured data. In Fig. 5., after applying this offset and with *s* = 0.002, it will be seen that apart from regions close to the junction with the side street the F1 model shows good agreement. If the phase

[1] Though in [28] Stadiou Street is called a parallel street in the configuration of Fig. 1 it is properly called a side street, as there is a direct line-of-sight from the position of the transmitting vehicle along the road leading to Stadiou Street

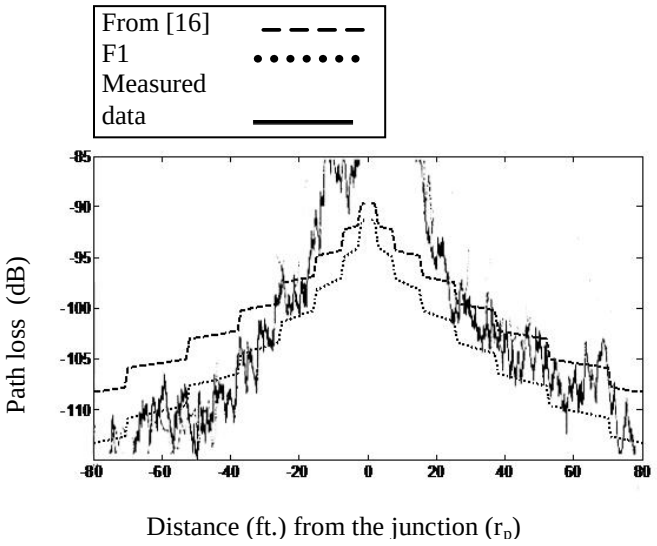

Fig. 5. Comparison of the equations for side-street path loss, from [16] and the revised equation (F1) including accurate calculation of propagation distance, 'foliage' effect, with measured data from [28], settings — frequency = 1.8 GHz, r_m = 110 m, W_m = 20 m, W_s = 26 m, s = 0.002

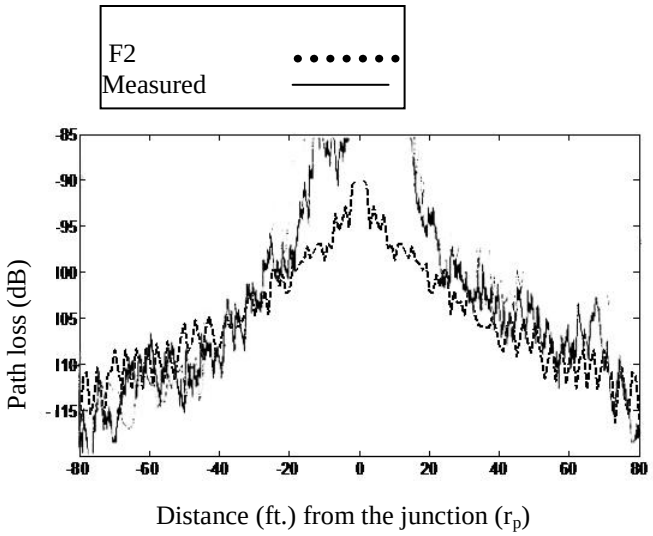

Fig. 6. Comparison of the equations for side-street path loss, the revised equation (F2) including accurate calculation of propagation distance, 'foliage' effect, and phase change, with measured data from [28], settings — frequency = 1.8 GHz, r_m = 110 m, W_m = 20 m, W_s = 26 m, s = 0.002

factors are included with the F2 model, Fig. 6, then the comparison with the measured data is also good.

B. LOS modeling

Apart from the 'foliage' effect, which we also employ for LOS modeling, in [21] the position of the breakpoint (distance when signal power changes from being proportional to r^{-2} to r^{-4}, where r is the distance from the transmitter vehicle) is adjusted by raising the effective ground-level according to traffic density in the two-ray ground propagation model for path loss, which is quoted here (before adjustment) for the convenience of the reader:

$$L(r) = \left(\frac{\lambda}{4\pi}\right)^2 \left| \frac{e^{-ikr_t}}{r_t} + R\frac{e^{-ikr_r}}{r_r} \right|^2 \tag{19}$$

where r_t is the direct optical path length from transmitter aerial to receiver aerial, r_r is the optical path length from the transmitter aerial via reflection from the ground to the receiver aerial, R is now the reflection coefficient. If the adjustment to ground level is h_0, then

$$r_r = \sqrt{r^2 + ((h_t - h_0) + (h_r - h_0))^2}\ , \tag{20}$$

where h_t and h_r are respectively the heights of the transmitter and receiver aerials respectively, with r the distance between transmitter and receiver vehicles. The breakpoint position is adjusted accordingly as

$$b_t = \frac{4(h_t - h_0) + (h_r - h_0)}{\lambda}, \tag{21}$$

where λ is the wavelength. However, changing the height of the aerials by a constant amount implies that traffic density is uniform, whereas simulation study has suggested [8] that there is a clustering of cars at intersections, especially when traffic lights are present. In [8], a mobility model dependent polynomial curve which depends on traffic density was fitted to empirical data. In Fig. 7, a 4th order polynomial has been fitted to this data, with the order chosen as a compromise between accuracy and computational complexity when applied in a simulation. For completeness, this curve is reported in (22).

$$CDF(x) = -265.27e-9x^4 + 39.88e-6x^2 - 2.15e-3x^2 + 60.13e-3x + 32.06e-3 \tag{22}$$

From this curve it is possible to probabilistically weight the calculation according to the probability that a car is present and acts as the reflecting surface at the crossover point (point of reflection of the ground ray) and the probability that the road surface forms the reflection surface. Equation (18) depends for this effect on the traffic density and, therefore, any probability is weighted by a normalized traffic density. Before normalization, we name the traffic density categories as: traffic high 4 cars/street segment, medium 3 cars/street segment, low 2 cars/street segment, and very low 1 car/street segment. A street segment is bounded by two junctions. Therefore, the second term in parentheses in (17) becomes:

$$P_1R_1\frac{e^{-ikr}}{r} + P_2R_2\frac{e^{-ikr_c}}{r_c} \tag{23}$$

where P_1 and P_2 are respectively the probabilities of a car being present and absence at the crossover point; and $R_1(\theta)$, $R_2(\theta)$, are respectively the reflection coefficients for the material of a car and the material of the road surface, which are dependent on the angle of incidence θ for constant frequency. Distance r is the distance travelled by a reflected ray from the ground, which is found in the normal way for the

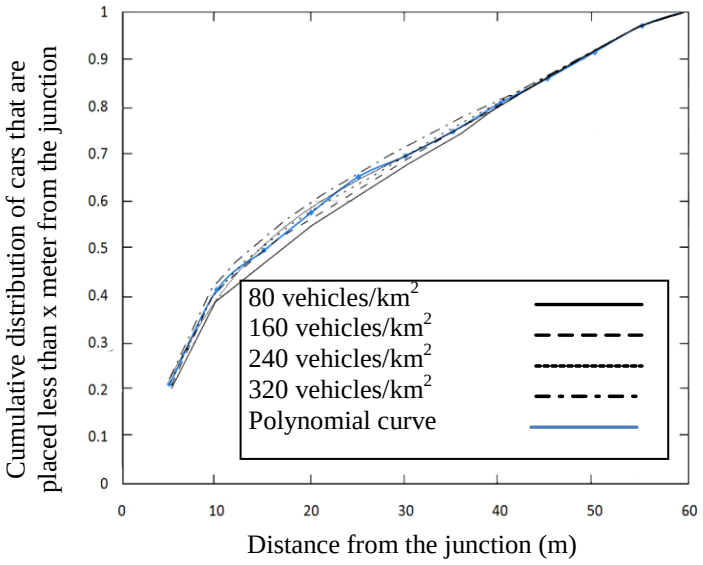

Fig. 7. Polynomial fit to CDF of cars from a junction, according to simulations conducted in [8], with order 4 polynomial fit.

two-ray model. However, r_c is the distance traveled by a ray reflected at the average height of a car above the ground (compare with [21]). Adjustment is also made in simulation for the fact that a car is not a point but extends on either side of the crossover point. An equation [29] for the reflection coefficient is:

$$R(\theta) = \frac{\cos\theta - at}{\cos\theta + at} \tag{24}$$

where a =1 for horizontal polarization and $a = \frac{1}{\eta_r^2}$ for vertical polarization (η_r is the relative impedance). If the angle of incidence is θ and $t = \sqrt{\eta_r^2 - \sin^2\theta}$. Typical conductivity, σ, for the low carbon steel of car bodies, the ground, and walls of tall buildings are respectively 6.8×10^{-6} S/m, from resistivity in [30], 0.005 mS/m [29], and 7 mS/m [10]. For the ground and walls it is possible to write

$$\eta_r^2 = \varepsilon_r = \varepsilon - i60\sigma\lambda \tag{25}$$

where ε_r is the relative dielectric constant and a typical value is $\varepsilon = 15$ [29]. (Notice that in the NLOS equations the same reflection coefficient as in [16] is employed by us.) However, an alternative form for low carbon steel is to use $\eta_r = \frac{\eta}{\eta_0}$ and the permittivity of the environment, $\eta = (1+i)\sqrt{\frac{\omega\mu}{2\sigma}}$, where μ is the permeability, and $\omega = 2\pi c/\lambda$, leading to a complex, frequency-dependent reflection coefficient. As horizontal polarization gives rise to oscillations in the value of the average signal strength prior to the break point in the two-ray model [26], vertical polarization was set.

We have applied a six-ray model with single- and double-reflection rays on either side of a street as well as the direct and ground reflected rays of the basic two-ray model. It is reported in [28] that this configuration of reflected rays in a LOS simulation gives best results. Given that it is reported [11] that positioning a vehicle in the middle of the road for ease of calculations has a minimal effect on the results and neglecting diffractions for LOS, the six-ray model results in the following estimates for single, R_s, and double, R_d, reflected propagation distances:

$$R_s = w_m / \cos\theta \tag{26}$$

where $\theta = \arctan(r_m / w_m)$.

$$R_d = 2(w_m / \cos\theta) \tag{27}$$

where $\theta = \arctan(r_m / (2w_m))$.

Notice that the inclusion of w_m in (27) means that the six-ray model is sensitive to street width, which is not the case for the two-ray model.

The adjusted LOS six-ray model taking account of differential ground reflection according to traffic density was plotted against data for Lexington Avenue and 22nd Street [22] as quoted in [10]. The transmitter and receiver aerial heights are respectively h_t and h_r are set according to the source data. In Fig. 8 for Lexington Avenue, the model generally follows the measured data more closely than the two-ray model does but at around $\pm$2000 ft, where there is destructive interference, when the model reports deeper drops in path loss. There may be at least two explanations for this discrepancy: 1) the results from [22] are averaged measurements and 2) the reflected paths are unlikely to exactly coincide in a real setting, even though in the mathematical model they do. The two-ray models discrepancies are across the range of measured data, which may be a problem in a simulation because a vehicle is unlikely to be positioned in exactly the area where the path loss is returned as low. Fig. 9 reports similar findings for 22nd Street. Differences in the response between Fig. 8 and Fig. 9 may lie in the distance between intersections, which are more frequent in Lexington Ave. than in 22nd Street.

In [31] an empirical model based on measured LOS data for Helsinki streets was given as:

$$L(r) = 40.3 + 23.4\log(r) \tag{28}$$

Fig. 10 compares the proposed model with two-ray model and the numerically derived fit from [31], when again the proposed model presents a reasonable compromise. The two-ray ground propagation model's behavior is characteristic of the oscillations *before* the breakpoint [21] (before which there is constructive and destructive interference between the two rays and after which the signal power falls off as r^{-4}).

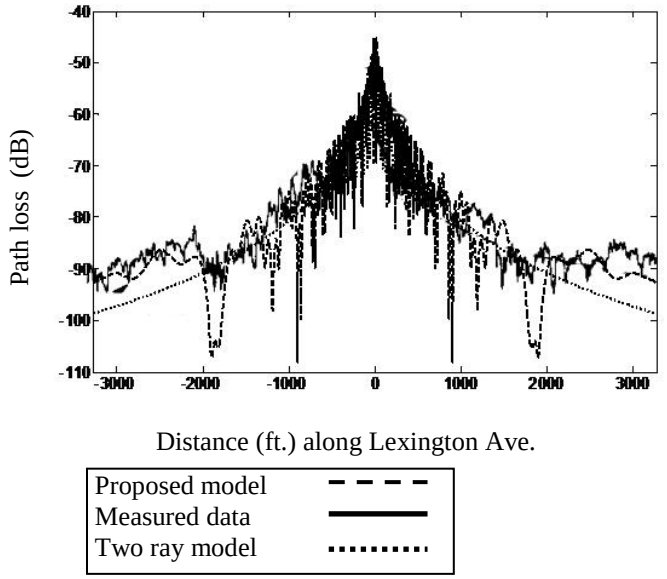

Fig. 8. Lexington Ave.: Proposed model with traffic effect, two-ray model and measured data – frequency = 900 MHz, ht =9.1m, hr =1.8 m, wm = 28.6 m, traffic density high, s = 0.001

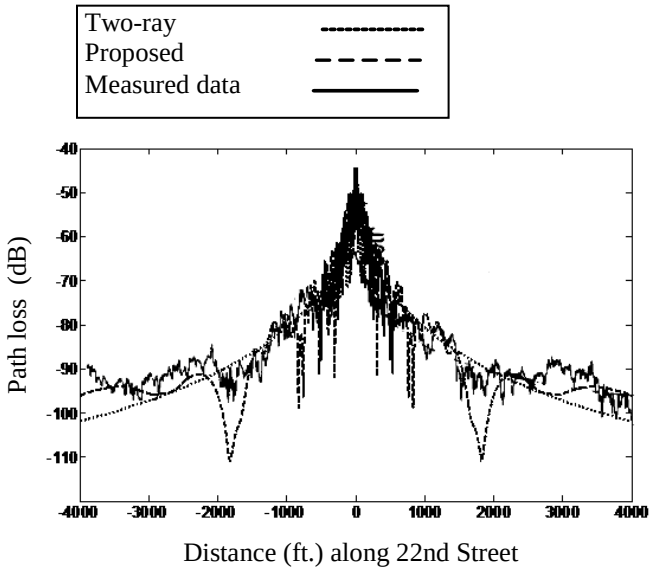

Fig. 9. 22nd Street: Proposed model with traffic effect, two-ray model and measured data – frequency = 900 MHz, ht =9.1m, hr =1.8 m, wm = 20.14 m, traffic density low, s = 0.001

C. Remarks on computation time

Though the issue of computational or implementation complexity is in general beyond the scope of this paper, we make a few remarks about this issue. Timings were taken on a PC with a dual-core Intel processor running at a nominal clock speed of 2.4 GHz for r_s ranging through ranging through 0 to 1524 m (the distance along 51st Avenue). In the mean, this took 0.0019 s for the equations in [16] and 0.0028 s for F1 in Section II.A, though adding phase results in a time of 0.0059 s. Calculating the two-ray ground propagation model took 0.0044 s. Therefore, using formula F1 with corrected propagation path distance and 'foliage effect' included does not increase the wall clock time by much over that of the equations of [16].

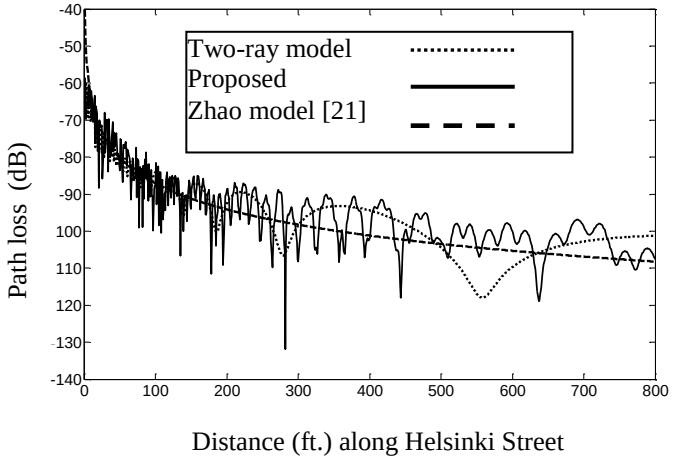

Fig. 10. Helsinki LOS street comparison of models: frequency = 5.3 GHz, ht =8 m, hr = 2, wm = 18 m, traffic density low, s = 0.002

TABLE I.
COMPARATIVE INDICATIVE TIMINGS FOR THE MODELS

Propagation model	*Mean (s)*	*Standard Deviation (s)*	*Maximum (s)*
Q.SUN [16]	0.0019	0.0051	0.0160
F1(Propagation path, scattering effects)	0.0028	0.0060	0.0160
F2 (Phase, propagation path, scattering)	0.0059	0.0076	0.0160
Two-ray model	0.0044	0.0070	0.0160
F1 (added Rayleigh fading)	0.0255	0.0076	0.0320
LOS	0.0243	0.0284	0.0297
Two-ray (added Rayleigh fading)	0.0282	0.0063	0.0320

In the case of LOS modelling, the proposed model took slightly less time in the mean compared to the two-ray model with additive Rayleigh fading but much more compared to the two-ray model alone. However, these timings should be taken as indicative rather than the absolute values that will be achieved. The results of timing experiments are presented in Table I. The results are subject to large deviations and the maxima are larger.

III. SIMULATION CASE STUDY

This simulation case study is not intended to be definitive but to show the consequences of incorporating the models developed in Section II compared to an elementary application of the two-ray model in which separate LOS and NLOS modeling does not occur. In the simulations with GloMoSim [19], a 1000×1000 m^2 area was defined and nodes (vehicles)

were initially randomly placed within the area. Results were averaged over 25 runs. Other settings for VanetMobiSim [9] to do with road cluster density, intersection density, lanes (2) and speeds are given in Table II. VanetMobiSim's simplest mobility model the Constant Speed Motion (CSM) does not produce realistic motions, and is included for comparison purposes only. The Intelligent Driver Model (IDM) accords with car following model developed elsewhere [32], based on live observations and also used in [33]. VanetMobiSim adds to this with modeling of intersection management (IDM-IM). The IDM-IM is extended to include lane change behavior or overtaking in the IDM-LC model.

The well-known Ad hoc On-Demand Distance Vector (AODV) [34] routing protocol was selected as a point of reference with the work of others. The Location-Aided Routing (LAR) protocol (version 1) [35] was also selected as it is able to restrict the area for route propagation by virtue of GPS information gathered from nodes in a VANET. The result is that LAR will incur less control packet overhead. The

TABLE II
VANETMOBISIM SETTINGS FOR ROAD LAYOUTS AND MOBILITY MODELS.

Global Parameters	
Simulation Time	900 s
Terrain Dimension	1000 x1000 m^2
Graph type	Manhattan grid model
Blocks	8 x 8
Block Size	125m
Number of Streets	81
Road width	20 m
Max. traffic lights	224
Time interval between traffic lights changing	45000 ms
Number of Lanes	2
Min. Stay	10 s
Max. Stay	100 s
Nodes (vehicles)	72, 144, 288, 432
Min. Speed	5 m/s (11 mph)
Max. Speed	36 m/s (80 mph)
Routing Protocol	AODV/LAR
Wireless Technology	IEEE 802.11p
CSM model	
Min. and max. pause time	0 s
IDM-LC Model	
Length of vehicle	5 m
Max. acceleration	0.6 m/s^2
Normal deceleration	0.5 m/s^2
Traffic jam distance	2 m
Node's safe time headway	1.5 s
Recalculation of movement parameters time	0.1 s
Safe deceleration	4 m/s^2
Politeness factor of drivers when changing lane	0.5
Threshold acceleration for lane change	0.2 m/s^2

advent of satellite navigation systems has indicated the benefits of GPS provision within vehicles (though see [36]) and if WLAN is available, GPS will also most likely be present. Despite its provenance LAR has been shown [37] to outperform many other recent protocols, except in respect to latency. The general advantage of position-aware routing algorithms in city VANETs is shown in [38].

As a default, a two-ray ground-propagation model with an omni-directional antenna height of 1.5 m at receiver and transmitter was selected for which the reflection coefficient was -0.7 [39], which is the same as that of asphalt at this frequency. The plane earth path loss exponent was set to 4.0 (for an urban environment rather than 2.4 for a highway [39]), with the direct path exponent set for free space propagation (2.0). As in IEEE 802.11p, transmission was at 5.9 GHz with a bandwidth of 10 MHz. Receiver sensitivity was set to -91 dBm. The transmission power of IEEE 802.11p was initially set to 23 dBm, (0.2 W), with lower power being favored to avoid the possible effect of interference at higher traffic densities. For example, in [40] transmission power was adaptively varied because at high traffic densities there are likely to be increased collisions and interference, excessive broadcasts, and too many routing paths.

IEEE 802.11p's robust Binary Phase Shift Keying (BPSK)[2] modulation mode was simulated at 1/2 coding rate, giving an effective data rate of 3 Mbps. Bit Error Rate (BER) modeling introduced a packet length dependency upon the form of modulation. Packet length was set to 500 B. Sources output to any one destination at a raw data rate of 72.7 kbps. With the inclusion of headers, this rate is still capable of transporting reasonable quality compressed Quarter Common Intermediate Format (QCIF) resolution video and 'lossy' audio. Source vehicles 1 and 2 simultaneously output in a logical mesh configuration to destination vehicles 3, 4, and 5, while vehicles 3, 4, and 5 also acted as sources and in a mesh configuration transmitted to destinations 6 and 7. In this way, vehicles 3, 4 and 5 are receivers and senders.

The proposed NLOS and LOS models are dynamically chosen in the simulator according to the position of the vehicles and the known layout of the buildings. For the proposed NLOS model, the path loss in (10) and (11) was set to -2 dB/reflection, which is the same value selected in [16]. In the proposed LOS model when applicable, values for reflection coefficients were the same as those reported in Section II. The average height of a car was set to 1 m and the length of a car was set to 5 m. Equation (20) relies on the mobility conditions set-up in the simulations. If these conditions are not available then it is possible to substitute a Normal CDF as an approximation to the clustering of cars at an intersection. In general, a Normal CDF may underestimate the number of cars at an intersection, though this aspect is outside the scope of this paper.

In Figs. 11a and 12a, the packet loss ratio (number of packets lost over number of packets sent) is compared against the proposed (called multiray in Figs. 11 and 12) and the two-ray ground propagation model of GloMoSim for the CSM and IDM-LC mobility models. From the Figures it is apparent that

[2] IEEE 802.11p also supports by default QPSK at 1/2 coding rate with an effective data rate of 6 Mbps.

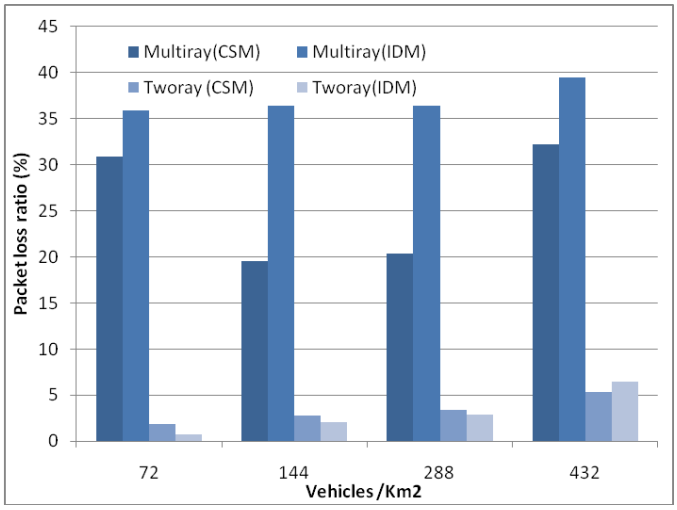

(a)

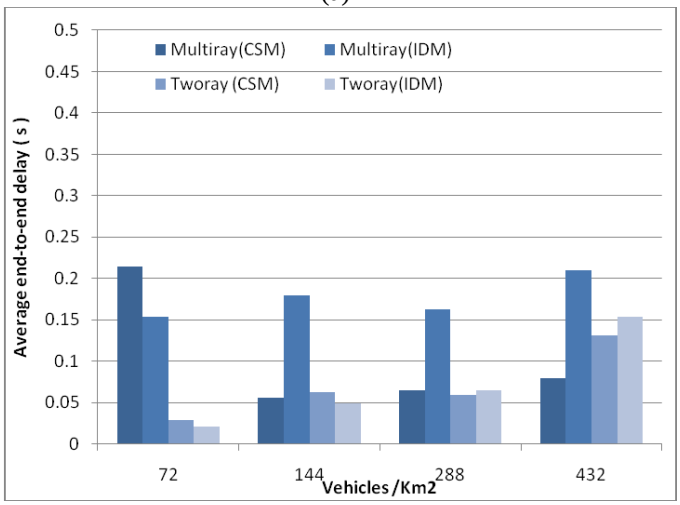

(b)

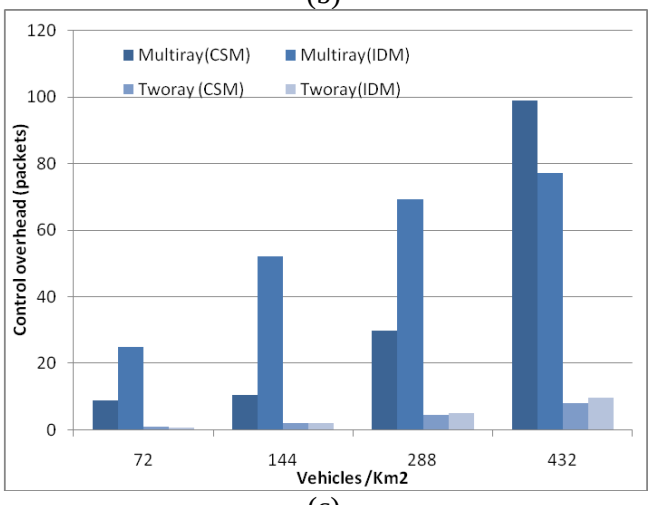

(c)

Fig. 11. (a) Packet loss (b) End-to-end delay, and (c) Packet overhead for differing traffic densities and driver mobility models according to propagation model with CSM and IDM-LC mobility models for the AODV protocol

the two-ray model consistently greatly underestimates the packet loss ratio. The ordering between the mobility models is also reversed, though this is not a strong effect. The main reason for the differences in path loss in the simulations appears to be that the impact of NLOS modeling tends to predominate. Though there is no direct comparison with the two-ray model, because it is a LOS model, the NLOS modeling by both [16] and the proposed improvements results in significantly more pessimistic estimates of path loss. Notice that LAR version 1 includes node (vehicle) proximity but not estimated distance in its routing procedures. Nevertheless, the number of hops in a route will tend to be reduced. However, in a simulation the LOS distance may be selected *even* when there may not be any physical LOS present, unless the simulation model is corrected. To check the transmitter power dependency the LAR results were repeated for network size 288 vehicles/km^2 with the IDM-LC mobility model, as reported for mean values in Table III. For the power range reported in Table III, as transmitter power increases the effect of path loss has a decreasing trend. This is not to say that the effects reported in [40] do not have an effect, but simply that, for this particular simulation case study, their influence is weak.

This result has important implications for real-time application types. For example, if retransmission is needed because of packet loss, this will affect end-to-end latency and for some real-time applications, which cannot tolerate delay, packet loss is acceptable *provided* it is below a given threshold. For example, a 10% packet loss threshold generally represents the difference between acceptable and unacceptable video quality at the receiver vehicle, before application-layer protection is applied. In this case study, end-to-end delay (Figs. 11b and 12b) and packet overhead (Figs. 11c and 12c) are both affected by the channel model, because of the effect on the routing protocol's ability to route, as of course it must exchange routing messages in the same way that the application must. Low network density also impedes the ability of the vehicles to communicate with each other, though this result is a by-product of the case study.

IV. Conclusion

Academic interest is naturally focused on competing claims of various innovations in routing protocols, MAC methods, and other worthy innovations. However, this is to neglect the requirement that application developers have in accurate assessment of the absolute gain in a particular performance metric or when comparing innovations the extent of the relative gain. In other words, an innovation may bring a gain but the gain may not be significant enough to warrant implementation. This may well explain why accurate simulation modeling of wireless VANETs is quite rightly emphasized by car manufacturers. This paper has sought to reinforce the increasingly detailed mobility models for urban environments with path-loss models for NLOS and LOS that remain computationally tractable and further improve predictions. It is in the NLOS modeling that the gain in accuracy seems most secure, as it was shown that it is possible to come closer to the measured data by a combination of improved propagation distance calculation and inclusion of the effect of roadside obstacles. In LOS modeling, inclusion of the

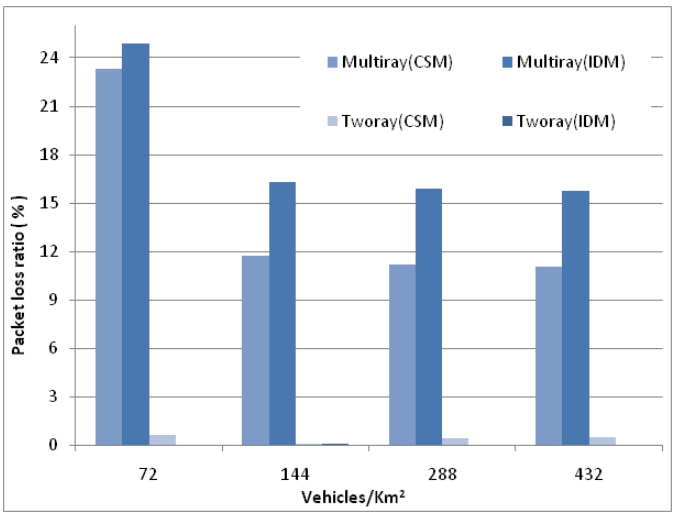

(a)

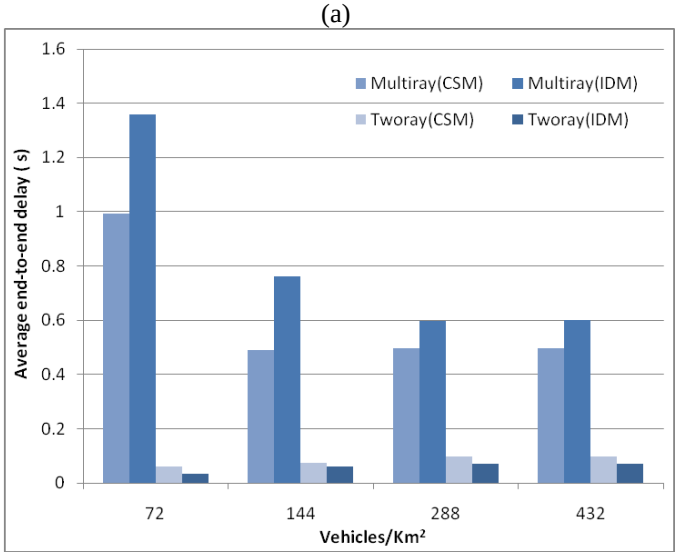

(b)

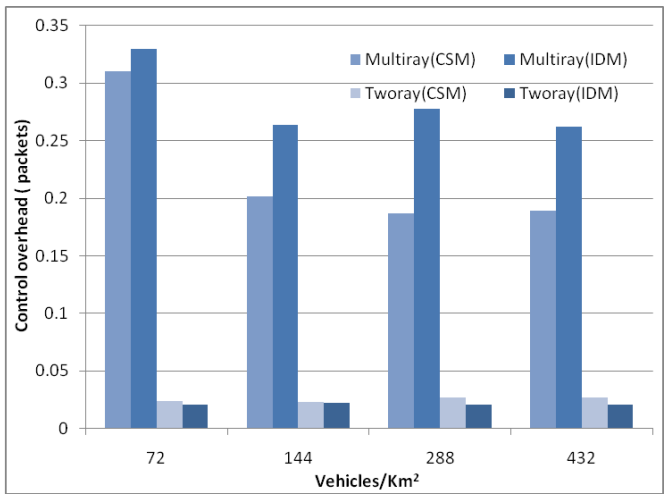

(c)

Fig. 12. (a) Packet loss (b) End-to-end delay, and (c) Packet overhead for differing traffic densities and driver mobility models according to propagation model with CSM and IDM-LC mobility models for the LAR protocol.

TABLE III
PACKET LOSS ACCORDING TO TRANSMITTER POWER

	Packet loss ratio (%) for LAR	
Power (dBm)	*Multi-ray IDM*	*Two-ray IDM*
15 (0.03 W)	41.2	6.8
20 (0.1 W)	20.4	0.3
23 (0.2 W)	15.9	0
30 (1 W)	5.2	0

implications of recent mobility models and reflection modeling must logically improve on a two-ray ground propagation model. An enhanced six-ray model also allows tracking of the profile of measured data for path loss, though mathematically modeling cannot come closer without detailed knowledge of building surfaces. For the same reason, the equations in this paper are not intended to be applied to predict detailed behavior in the field, as this is best accomplished by measurements. The formulas are, however, intended for incorporation into simulators, which can be used, for instance, to analyze the behavior of routing protocols within VANETs. Though the results for the ray-tracing, 'multi-ray' model is in general more pessimistic than the two-ray ground propagation model it is unlikely that they are too pessimistic. This is because the minimum number of reflections has been taken into account, whereas in reality building surfaces would not be flat resulting in more reflections not less.

REFERENCES

[1] S. M. Hur, S. Mao, Y. T. Hou, K. Nam, and J. H. Reed, "Exploiting location information for concurrent transmissions in multihop wireless networks," *IEEE Trans. on Vehicular Technol.*, vol. 58, no. 1, pp. 314-323, Jan. 2009.

[2] I. Sen and D. W. Matolak, "Vehicle-to-vehicle channel models for the 5-GHz band," *IEEE Transactions on Intelligent Transportation Systems*, vol. 9, no. 2, pp. 235-245, June 2008.

[3] M. Takai, J. Martin, and R. Bagrodia, "Effects of wireless physical layer modeling in mobile ad hoc networks," in *Proc. of Int'l. Symp. on Mobile Ad Hoc Networking and Computing*, Oct. 2001, pp. 87-94,

[4] M. Wellens, M. Petrova, J. Riihijärvi, and P. Mähönen, "Building a better mousetrap: Need for more realism in simulation," in *Proc. of 2nd Ann. Conf. on Wireless on Demand Network Syst. and Services*, Jan. 2005, pp. 150-157.

[5] F. J. Martinez, C.-K. Toh, J. C. Kano, C. T. Calafate, and P. Manzoni, "Realistic radio propagation models (RPMs) for VANET simulations," in *Proc. of IEEE Wireless Communs. and Networking Conf.*, 2009, pp. 1-6.

[6] I. Tan and A. Bahai, "Physical layer considerations for vehicular communications," in *VANET: Vehicular Applications and Inter-Networking Technologies*, J. Wiley and Sons, Chichester, UK, 2010, pp. 157-218.

[7] B. Liu, B. Khorashadi, H. Du, D. Ghosal., C-N. Chuah, and M. Zhang, "VGSim: An integrated networking and microscopic vehicular mobility simulation platform," *IEEE Communications Mag*., vol. 47, no. 5, pp. 134-141, May 2009.

[8] O. K. Tonguz, W. Viriyasitavat, and F. Bai, "Modeling urban traffic: A Cellular automata approach," *IEEE Communs. Mag*., vol. 47, no. 5, pp. 142-150, May 2009

[9] M. Fiore, J. Härri, F. Filali, and C. Bonnet, "Vehicular mobility simulation for VANETs," in *Proc. of 40th Annual Simulation Symposium*, March 2007, pp. 301-307.

[10] S. Y. Tan and H. S. Tan, "A microcellular communications propagation model based on the uniform theory of diffraction and multiple image theory," *IEEE Trans. on Antennas and Propagation*, vol. 44, no. 10, pp. 1317-1326, Oct. 1996.

[11] V. Erceg, S. Ghassemzadeh, M. Taylor, D. Li and D L. Schilling, "Urban/suburban out of sight propagation modelling," *IEEE Communs. Mag.*, vol. 30, no. 6, pp. 56-61, June 1992.

[12] H. R. Anderson, "A ray-tracing propagation model for digital broadcast systems in urban areas," *IEEE Trans. on Broadcasting*, vol. 39, no. 3, pp. 309-317, Sept. 1993.

[13] J. Oishi, K. Asakura, and T. Watanabe, "A communication model for inter-vehicle communication simulation systems based on properties of urban areas," *Int'l J. of Computer Science and Network Security*, vol. 6, no. 10, pp. 213-219, Oct. 2006.

[14] A. J. Goldsmith and L. J. Greenstein, "A measurement-based model for predicting coverage areas of urban microcells," *IEEE J. on Sel. Areas in Communications*, vol. 11, no. 7, pp. 1013-1023, Sept. 1993.

[15] F. Niu and H. L. Bertoni, "Path loss and cell coverage of urban microcells in high-rise building environments," *In Proc. of IEEE GLOBECOM*, Nov. 1993, pp. 266-270.

[16] Q. Sun, S. Y. Tan, and K. C. Ter, "Analytical formulae for path loss prediction in urban street grid microcellular environments," *IEEE Trans. on Vehicular Technol.*, vol. 54, no. 4, pp. 1251-1258, July 2005.

[17] T. K. Sarkar, Z. Ji, K. J. Kim, A. Medouri, and M. Salazar-Palma, "A survey of various propagation models for mobile communication," *IEEE Antennas Propag. Mag.*, vol. 45, no. 3, pp. 51-82, 2003.

[18] M. Torrent-Moreno, S. Corroy, F. Shmidt-Eisenlohr, and H. Hartenstein, "IEEE 802.11-based one-hop broadcast communications: Understanding success and failure under different propagation environments," in *Proc. of Int. Workshop on Modeling Analysis and Simulation of Wireless and Mobile Systems*, pp. 68-77, 2006.

[19] X. Zeng, R. Bagrodia, and M. Gerla, "GloMoSim: A library for parallel simulation of large-scale wireless networks," in *Proc. of 12th Workshop on Parallel and Distributed Simulations*, May 1998, pp. 154-161.

[20] F. Bai, N. Adagopan, and A. Helmy, "IMPORTANT: A framework to systematically analyze the Impact of Mobility on Performance of routing protocols over Adhoc NeTworks*,"* in *Proc. of IEEE INFOCOM*, Apr. 2003, pp. 825-835.

[21] Y. Oda, K. Tasunekawa, and M. Hata, Advanced LOS path-loss model in microcellular mobile communications," *IEEE Trans. on Vehicular Technol*., vol. 49, no. 6, pp. 2121-2125, Nov. 2000.

[22] A. J. Rustako Jr., N. Amitsay, G. J. Owens, and R. S. Roman, "Radio propagation at microwave frequencies for line-of-sight microcellular mobile and personal communications," *IEEE Trans. on Vehicular Technol.*, vol. 40, no. 1, pp. 203-210, Feb. 1991.

[23] ASTM Committee on Vehicle-Pavement Systems, *ASTM E2213-03, 2003, Standard specification for telecommunications and information exchange between roadside and vehicular systems — 5 GHz band Dedicated Short Range Communications (DSRC) Medium Access Control (MAC) and Physical Layer (PHY) specifications*, 2003.

[24] D. Jiang and L. Delgrossi, "IEEE 802.11p: Towards an international standard for wireless access in vehicular environments," in *Proc. of IEEE Vehicular Technol. Conf*., May 2008, pp. 2036-2040.

[25] L. Cheng, B. E. Henty, R. Cooper, D. D. Standl, and F. Bai, "A measurement study of time-scaled 802.11a waveforms over the mobile-to-mobile vehicular channel at 5.9 GHz," *IEEE Communications Mag.*, vol. 46, no. 5, pp. 84-91, 2008.

[26] R. Nagle and S. Eichler, "Efficient and realistic mobility and channel modeling for VANET scenarios using OMNeT++ and INET-framework," in *Proc. of OMNeT++ Workshop*, article no. 18, 2008.

[27] L. Denegri, L. Bixio, F. Lavagetto, A. Iscra, and C. Braccini, "An analytical model of microcellular propagation in urban canyons," in *Proc. of Vehicular Technol. Conf.*, pp. 402-406, April 2007.

[28] N. Papakadis, A. G. Kanatas, and P. Constantinou, "Microcellular propagation and simulation at 1.8 GHz in urban radio environment," *IEEE Trans. on Vehicular Technol.*, vol. 47, no. 3, pp. 1012-1026, Aug. 1998.

[29] H. H. Xia, H. L. Bertoni. L. R. Maciel, "Radio propagation characteristics for line-of-sight microcellular and personal communications," *IEEE Trans. on Antennas and Propagation*, vol. 41, no. 10, pp. 1439-1447, Oct. 1993.

[30] American Society of Metals (ASM) Handbook Committee, *Metals Handbook*, ASM, Metals Park, OH, 1978.

[31] X. Zhao, T. Rautiainen, K. Kalliola, and P. Vainikainen, "Path-loss models for urban microcells at 5.3 GHz," *IEEE Antennas and Wireless Propagation Letters*, vol. 5, pp.152-154, 2005.

[32] M. Treiber, A. Henneke, and D. Helbing, "Congested traffic states in empirical observations and microscopic simulations," *Phys. Rev. E*, vol. 62, no. 2, pp. 1805-1824, Aug. 2000.

[33] A. Kesting, M. Treiber, and D. Helbing, "Connectivity statistics of store-and-forward inter-vehicle communication," *IEEE Transactions on Intelligent Transportation Systems*, vol. 11, no. 1, pp. 172-181, Mar. 2010.

[34] C. E. Perkins and E.M. Royer, "Ad-hoc on-demand distance vector routing algorithms for mobile wireless networks," in *Proc. of IEEE Workshop on Mobile Computing Systems and Applications*, pp. 90-100, Feb. 1999.

[35] Y. B. Ko and N. H. Vaidya, "Location-Aided-Routing (LAR) in mobile ad-hoc networks," in *Proc. of ACM/IEEE MOBICOM*, pp. 66-75, Oct. 1998.

[36] M.M. Drawil and O. Basir, "Intervehicle-communication-assisted localization," *IEEE Transactions on Intelligent Transportation Systems*, vol. 11, no. 3, pp. 678-691, Sept. 2010.

[37] N. N. Qadri and A. Liotta, "A comparative analysis of routing protocols for MANETs," in *Proc. of IADIS Int'l. Conf. on Wireless Applications and Computing*, Nov. 2008.

[38] C. Lockert, H. Hartenstein, J. Tian, H. Füßler, D, Hermann, and M. Mauve, "A routing strategy for vehicular ad networks in city environments," in *Proc of the IEEE Intelligent Vehicles Symposium*, pp. 156-161, 2003.

[39] L. Stibor, Y. Zhang, and H.-J. Reumann, "Evaluation of communication distance in a vehicular ad hoc network using IEEE 802.11p*,"* in *Proc. of Wireless Communication and Networking Conf.*, pp. 254-257, Mar. 2007.

[40] M. Artimy, "Local density estimation and dynamic transmission range assignment in vehicular ad hoc networks," *IEEE Transactions on Intelligent Transportation Systems*, vol. 8, no. 3, pp. 400-412, Sept. 2007.